

Tracking neighboring quasi-satellite orbits around Phobos

Muralidharan, Vivek; Weiss, Avishai; Kalabic, Uros

TR2020-102 July 16, 2020

Abstract

We consider the orbital maintenance problem on a quasi-satellite orbit about the Martian moon, Phobos. The orbit is computed using a high-fidelity ephemeris model so that the major sources of disturbances are due to measurement error. Two types of orbit maintenance schemes are considered. The first is based on asymptotically tracking the desired trajectory and the second is based on stabilizing to the manifold of trajectories that share the same Jacobi constant as the reference trajectory. The latter can be done because trajectories with the same Jacobi constant are in the neighborhood of one another. The results show that the trajectory-tracking scheme has lower fuel consumption when tracking must be precise and that the approach of stabilizing to a manifold has better fuel consumption at the expense of tracking.

World Congress of the International Federation of Automatic Control (IFAC)

This work may not be copied or reproduced in whole or in part for any commercial purpose. Permission to copy in whole or in part without payment of fee is granted for nonprofit educational and research purposes provided that all such whole or partial copies include the following: a notice that such copying is by permission of Mitsubishi Electric Research Laboratories, Inc.; an acknowledgment of the authors and individual contributions to the work; and all applicable portions of the copyright notice. Copying, reproduction, or republishing for any other purpose shall require a license with payment of fee to Mitsubishi Electric Research Laboratories, Inc. All rights reserved.

Tracking neighboring quasi-satellite orbits around Phobos[★]

Vivek Muralidharan^{*} Avishai Weiss^{**} Uroš Kalabić^{**}

^{*} *School of Aeronautics and Astronautics, Purdue University, West Lafayette, IN 47907, USA (e-mail: muralidv@purdue.edu)*

^{**} *Mitsubishi Electric Research Laboratories, Cambridge, MA 02139, USA (e-mails: weiss,kalabic@merl.com)*

Abstract: We consider the orbital maintenance problem on a quasi-satellite orbit about the Martian moon, Phobos. The orbit is computed using a high-fidelity ephemeris model so that the major sources of disturbances are due to measurement error. Two types of orbit maintenance schemes are considered. The first is based on asymptotically tracking the desired trajectory and the second is based on stabilizing to the manifold of trajectories that share the same Jacobi constant as the reference trajectory. The latter can be done because trajectories with the same Jacobi constant are in the neighborhood of one another. The results show that the trajectory-tracking scheme has lower fuel consumption when tracking must be precise and that the approach of stabilizing to a manifold has better fuel consumption at the expense of tracking.

Keywords: Aerospace; space exploration and transportation; guidance, navigation and control of vehicles; station-keeping; quasi-satellite orbits.

1. INTRODUCTION

Our understanding of Mars, the planet most similar to our own, is greatly enhanced with the sending of spacecraft to visit the red planet. Previous Mars missions include the Mars Orbiter Mission (MOM) (Helfrich et al., 2015), the Mars Reconnaissance Orbiter (MRO) (Zurek and Smrekar, 2007), and the Mars Atmosphere and Volatile Evolution (MAVEN) mission (Jakosky et al., 2015). In these missions the spacecraft observed Mars, so the orbital design of these missions was based on a two-body conic orbit structure; however, when studying one of the Martian moons, it is no longer possible to restrict the orbital design with the two-body assumption. This is because the moons have a relatively small mass and therefore the primary body, *i.e.*, Mars, still has a dominant gravitational effect even on spacecraft that are in close proximity to a moon.

In this work, we consider the problem of orbital tracking in a mission to Phobos. The work is motivated by the planned Mars Moon Exploration (MMX) mission (Campagnola et al., 2018; Çelik et al., 2019) that will study the origins of the moon. The mass ratio of Phobos is $\mu = 1.6606 \times 10^{-8}$, making it so small relative to Mars that the orbits where the influence of Mars is negligible are smaller than Phobos itself. For this reason, it becomes necessary to perform orbital design under the three-body assumption, specifically using the restricted three-body model in which the effect of gravitation due to the spacecraft is assumed to be negligible. By assuming that the dominant bodies orbit their barycenter in circular orbits, the problem of finding a closed orbit for the spacecraft is termed the circular restricted three-body problem (CR3BP). Multiple

solutions exist to the CR3BP, and the one of interest to us is called the quasi-satellite orbit (QSO), a quasi-periodic orbit that resembles an ordinary, periodic, two-body satellite orbit. In the case of the Mars-Phobos system, the QSO is a good choice of orbit around Phobos due to its distance from Phobos being far enough to ensure that the spacecraft does not come into contact with its surface while being near enough to make detailed observations.

We consider two schemes to track the Mars-Phobos QSO. The first is based on a conventional trajectory-tracking method based on the solution to a tracking linear quadratic regulator (LQR) problem (Stengel, 1994). The unique aspect of the scheme proposed here is that the state-penalty matrix is set to equal the structure of the *a priori* state uncertainty matrix. The second is an alternative based on stabilizing to a neighborhood of the reference QSO, specifically to tracking an orbit with the same constant of integration as the reference. This constant of integration, called the Jacobi constant, is a measure of the energy of the orbit. QSOs with the same Jacobi constant are guaranteed to be close to one another and therefore staying at this energy level is guaranteed to keep the resulting trajectory in a neighborhood of the reference (McCarthy, 2019). This scheme is similar to methods that use space manifold dynamics (Perozzi and Ferraz-Mello, 2016) to design transfer orbits and are not typically used for trajectory tracking. In reality, QSOs in the CR3BP are not directly implementable, but it is well-known that a QSO in the CR3BP can be grown from the closed orbit solution of the CR3BP (Capdevila, 2016; McCarthy, 2019). Similarly, although constant in the case of the CR3BP, in reality the Jacobi energy measure is not a constant but is nevertheless tightly bounded.

[★] This work was supported by Mitsubishi Electric Laboratories.

We perform Monte Carlo simulations to determine fuel consumption of both approaches corresponding to different optimization parameters. The results show that both approaches can be tuned to significantly reduce fuel consumption. The neighborhood station-keeping approach must be modified to ensure better tracking of the reference QSO by adding an additional quadratic penalty term. In this case, the fuel consumption rises rapidly. We therefore recommend that the approach should be used primarily for orbital maintenance in situations where precise station-keeping is not required, such as in emergencies where fuel consumption is paramount.

The rest of the paper is structured as follows. Section 2 presents the determination of the QSO. Section 3 presents the station-keeping strategies. Section 4 presents numerical results. Section 5 is the conclusion.

2. QUASI-SATELLITE ORBIT AROUND PHOBOS

Solutions to the two-body problem are conic sections representing a spacecraft's path around one gravitational body. Once the spacecraft motion is significantly away from the primary gravitational body, its motion is influenced by the gravitation of other celestial bodies. Solutions to the circular restricted three body problem (CR3BP) are a better approximation of spacecraft motion, as they consider the spacecraft motion subject to gravitational forces in a sun-planet or planet-moon system, where both bodies are assumed to be moving in a circular path about the barycenter.

In this work, we consider the Mars-Phobos system, which has a mass ratio $\mu = 1.6606 \times 10^{-8}$, meaning that the mass of Phobos is a fraction μ of the Mars-Phobos system. The equations of motion for this system are given by,

$$\ddot{x} - 2\dot{y} - x = -\frac{1-\mu}{r_{13}^3}(x+\mu) - \frac{\mu}{r_{23}^3}(x-1+\mu), \quad (1a)$$

$$\ddot{y} + 2\dot{x} - y = -\frac{1-\mu}{r_{13}^3}y - \frac{\mu}{r_{23}^3}y, \quad (1b)$$

$$\ddot{z} = -\frac{1-\mu}{r_{13}^3}z - \frac{\mu}{r_{23}^3}z, \quad (1c)$$

where,

$$r_{13} = \sqrt{(x+\mu)^2 + y^2 + z^2},$$

$$r_{23} = \sqrt{(x-1+\mu)^2 + y^2 + z^2},$$

and x, y, z are defined in the rotating coordinate system centered at the barycenter of the planet-moon system as non-dimensionalized, normalized quantities according to Szebehely (1967). The x -axis points in the direction of Phobos, the z -axis points in the direction of the angular momentum of system around its barycenter, and the y -axis completes the right hand coordinate system. An energy-like constant of integration that exists in the CR3BP is called the Jacobi constant C , which is given by (Szebehely, 1967),

$$C = \frac{2(1-\mu)}{r_{13}} + \frac{2\mu}{r_{23}} + (x^2 + y^2) - (\dot{x}^2 + \dot{y}^2 + \dot{z}^2). \quad (2)$$

Limit-cycle solutions to (1) are termed orbits, for which there exist numerous families. Within the Sun-Earth and Earth-Moon systems, the class of orbits that are typically preferred are the Lyapunov and halo orbits (Shirobokov

et al., 2017) due to the proximity to the secondary body as well as their stability properties and structures that make it suitable for conducting scientific experiments and making observations of the secondary body. While these two types of orbits do exist in the Mars-Phobos system, a majority of them pass through the surface of Phobos, making them infeasible for a sufficiently long-term mission. Alternatively, in the same system, there exist close-to-stable, planar orbits called distant retrograde orbits (DROs) and these keep the spacecraft at a relatively far distance from Phobos. These orbits are planar and therefore not ideal candidates for missions seeking to observe the entire surface of the moon. However, three-dimensional, quasi-periodic structures, called quasi-satellite orbits (QSOs), exist in the neighborhoods of DROs and these have been explored as candidate trajectories for potential missions (McCarthy, 2019). In this work, we consider such an orbit of approximate dimension 100km-by-200km-by-60km, which is an orbit that provides good coverage of Phobos while remaining sufficiently far from the moon, with an orbital period that is approximately equal to the time period of Phobos orbiting around Mars.

Orbit determination The determination of our QSO is performed by modifying a DRO. It is difficult to directly construct a QSO and, therefore, we begin by following the computational procedure of Capdevila (2016) to generate a family of DRO orbits with approximate dimension of 100km-by-200km in the x - y plane. These DROs are stacked on top of each other sequentially in time, with each revolution discretized into 4 patch points (Howell and Pernicka, 1988). The multiple-shooting continuation scheme of Muralidharan (2017) is then implemented with the additional constraint of a fixed z -coordinate of the first patch point, resulting in a continuous, free trajectory. The solution is then used as an initial guess to a new multiple-shooting problem, with higher target z -amplitude, and this is repeated until the z -coordinate of the first patch point is equal to the desired 60km. The result is the orbit shown in Fig. 1.

The QSO trajectory that we obtain is free under the assumptions of the CR3BP. However, due to the disturbances of other celestial bodies, the trajectory is not free in reality. To compute the true, free trajectory, we use a high-fidelity ephemeris models `mar097` and `de421` (Jacobson et al., 2018; Folkner et al., 2009) to propagate the dynamics. We use the solution from the previous step, discretized at 4 patch points per revolution, as an initial guess to a new multiple-shooting scheme that gives a continuous, and truly free, trajectory.

3. STATION-KEEPING

Although the orbit is free, system disturbances, the dominant one of which is estimation error (Muralidharan et al., 2020), cause deviations of the spacecraft from the desired path. For this reason, we implement station-keeping schemes that ensure we remain close to the desired trajectory. In this section, we introduce two such schemes for comparison: a trajectory-tracking scheme which ensures close tracking and a manifold-stabilization scheme that guarantees that the satellite remain in the neighborhood of the desired orbit.

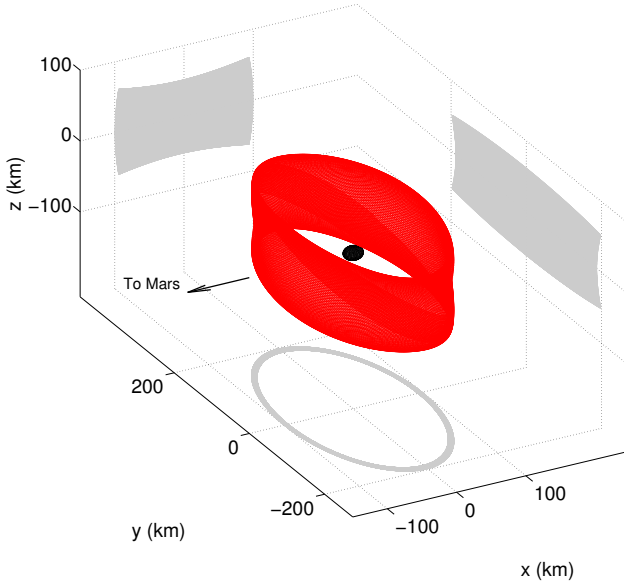


Fig. 1. QSO of size 100km x 200km x 60km; because it evolves from the DRO, the trajectory moves in the clockwise direction when viewed in the $x - y$ plane

3.1 Trajectory-tracking

In the neighborhood of the trajectory, we can approximately model the dominant dynamics with the time-varying linear system,

$$\delta \mathbf{x}_{k+1} = \mathbf{A}_k \delta \mathbf{x}_k + \mathbf{B}_k \Delta \mathbf{v}_k, \quad (3)$$

where $\delta \mathbf{x}_k = \mathbf{x}(t_k) - \mathbf{x}_0(t_k)$, $\mathbf{x}(t_k)$ is the six-dimensional actual state and $\mathbf{x}_0(t_k)$ is the reference state measured at the discretization time-step t_k , and $\Delta \mathbf{v}_k$ is the three-dimensional vector of an impulsive maneuver, *i.e.*, instantaneous velocity change at t_k ; the system matrices are obtained numerically. To maintain orbit, we minimize the cost functional,

$$\delta \mathbf{x}_N^T \mathbf{P}_N \delta \mathbf{x}_N + \sum_{k=0}^{N-1} \delta \mathbf{x}_k^T \mathbf{Q}_k \delta \mathbf{x}_k + \Delta \mathbf{v}_k^T \mathbf{R}_k \Delta \mathbf{v}_k, \quad (4)$$

over the mission duration $[t_0, t_N]$. The solution to this LQR problem is given by (Stengel, 1994),

$$\Delta \mathbf{v}_k = -\mathbf{K}_k \delta \mathbf{x}_k, \quad (5)$$

where \mathbf{K}_k is the time-dependent gain matrix that satisfies,

$$\mathbf{K}_k = (\mathbf{R}_k + \mathbf{B}_k^T \mathbf{P}_{k+1} \mathbf{B}_k)^{-1} \mathbf{B}_k^T \mathbf{P}_{k+1} \mathbf{A}_k, \quad (6)$$

and \mathbf{P}_k satisfies the discrete algebraic Riccati equation,

$$\mathbf{P}_k = \mathbf{Q}_k + \mathbf{A}_k^T \mathbf{P}_{k+1} \mathbf{A}_k - \mathbf{A}_k^T \mathbf{P}_{k+1} \mathbf{B}_k \mathbf{K}_k, \quad (7)$$

for $k = 0, \dots, N-1$.

The choice of penalty matrices \mathbf{P}_N , \mathbf{Q}_k , and \mathbf{R}_k should be made judiciously. To do this, we begin by noting that, since the orbit computation is based on highly accurate data, the major source of disturbance is the noisy estimates of the spacecraft position and velocity. We also present the covariance of this measurement error at time t_k ,

$$\mathbf{W}_k = \mathbb{E}[(\hat{\mathbf{x}}(t_k) - \mathbf{x}(t_k))(\hat{\mathbf{x}}(t_k) - \mathbf{x}(t_k))^T],$$

where $\hat{\mathbf{x}}(t_k)$ is the state measurement. We are interested in the error with respect to the desired trajectory, whose *a posteriori* covariance is given by,

$$\begin{aligned} \mathbf{S}_k &= \mathbb{E}[(\hat{\mathbf{x}}(t_k) - \mathbf{x}_0(t_k))(\hat{\mathbf{x}}(t_k) - \mathbf{x}_0(t_k))^T], \\ &= \mathbf{W}_k + \mathbb{E}[(\mathbf{x}(t_k) - \mathbf{x}_0(t_k))(\mathbf{x}(t_k) - \mathbf{x}_0(t_k))^T], \end{aligned}$$

under the assumption that the trajectory-tracking and measurement errors are uncorrelated, which is true if and only if their initial errors are uncorrelated. The predicted, *a priori* covariance evolves according to the closed-loop system dynamics,

$$\mathbf{S}_{k+1} = \hat{\mathbf{A}}_k \mathbf{S}_k \hat{\mathbf{A}}_k^T + \mathbf{W}_{k+1}. \quad (8)$$

for $k = 0, \dots, N-1$, where $\hat{\mathbf{A}}_k = \mathbf{A}_k - \mathbf{B}_k \mathbf{K}_k$.

Since we wish that the spacecraft track the trajectory as closely as possible, we set $\mathbf{Q}_k = \mathbf{S}_k$ for all k . This is true because \mathbf{S}_k is a measure of our confidence in our estimate; the higher the confidence, the less we need to penalize that particular state. Since there is no preferred thruster direction, the penalty on control is chosen to be constant and equal in all directions, giving $\mathbf{R}_k \equiv r \mathbf{I}_3$ for some $r > 0$. Since we are interested in low-energy solutions, we set r to be a substantially large number. However, we note that r cannot be too large as this would eventually cause poor enough tracking of the trajectory to invalidate the assumption of linearity, causing the satellite to drift off into space. Our choice of r is informed through simulation.

We solve (6)-(8) for the optimal control gain \mathbf{K}_k . To find a solution, we note that (7) is stable backwards in time with required final condition \mathbf{P}_N , while (8) is stable forwards in time with required initial condition \mathbf{S}_0 . We find the solution by initially setting $\mathbf{P}_k = \mathbf{S}_k \equiv \mathbf{S}_0$ and propagating (8) forwards and (7) backwards until converging to a solution, setting $\mathbf{Q}_k = \mathbf{S}_k$ for $k = 0, \dots, N-1$ and $\mathbf{P}_N = \mathbf{S}_N$ every time after completing the forward pass. Note that \mathbf{S}_0 is an *a posteriori* covariance and may be the output of a filter, or solely due to error inherent in the device used for measurement.

3.2 Neighborhood station-keeping

Since it may not be a mission requirement that the spacecraft precisely follow a prescribed orbital trajectory, we introduce a method that ensures that the satellite remains near Phobos but not at a specific location along a desired orbit. Loosening the tracking constraint allows us to reduce a significant amount of fuel while still allowing close flybys of the moon. In particular, our scheme is based on the realization that a family of orbits with the same Jacobi constant have distances from the secondary body that, while not the same across the family, do not deviate greatly from one another. For this reason, instead of tracking a prescribed trajectory, we impose the tracking of this energy constant.

Let C_d be the Jacobi constant of the QSO trajectory obtained in the CR3BP. It has been shown that the Jacobi constants of orbits computed in the CR3BP and extended to more general assumptions are related to each other and evolve on a shared manifold (Kolemen et al., 2007). Therefore, a spacecraft that deviates from the reference path can be returned to a similar orbit in the neighborhood of the original orbit.

The approach we propose is a receding horizon controller that determines the predicted sequence of $\Delta \mathbf{v}_{i|k}$ that ensures the spacecraft will track a new trajectory that

Table 1. 30-day trajectory tracking station-keeping cost for different choices of r

r	CR3BP		Ephemeris	
	Mean (m/s)	1 σ (m/s)	Mean (m/s)	1 σ (m/s)
10^{-4}	9.40	0.85	9.34	0.98
10^{-3}	6.85	0.59	6.66	0.58
10^{-2}	3.82	0.29	3.64	0.29
10^{-1}	1.99	0.19	1.95	0.19
10^0	1.13	0.16	1.14	0.16

is close to the nominal and that converges at the end of the time-horizon to the desired Jacobi constant C_d . The control is determined by solving an optimal control problem over the finite-time horizon N ,

$$\min_{\Delta \mathbf{v}_{i|k}, T_{i|k}} \alpha \sum_{i=0}^{N-1} \xi_i \|\Delta \mathbf{v}_{i|k}\| + (1 - \alpha) (\|\mathbf{r}_{i|k}\|_{\mathbf{W}_r}^2 + \|\mathbf{v}_{i|k}\|_{\mathbf{W}_v}^2) \quad (9a)$$

$$\text{sub. to } t_{0|k} = 0, \quad (9b)$$

$$\Delta \mathbf{v}_{i|k} = \Delta \mathbf{v}(T_{i|k}), \quad i = 0, \dots, N - 1, \quad (9c)$$

$$C_{N|k} = C_d. \quad (9d)$$

and setting the control,

$$\Delta \mathbf{v}_k = \Delta \mathbf{v}_{0|k}, \quad (10)$$

and updating the control at time $T_{1|k}$, where $\mathbf{r}_{i|k}$ and $\mathbf{v}_{i|k}$ are the position and velocity state, respectively, at time t_{k+i} computationally determined at time t_k ; similarly, $\Delta \mathbf{v}_{i|k}$ is the value of $\Delta \mathbf{v}_{k+i}$, computationally determined at time t_k ; α , ξ_i , \mathbf{W}_r , \mathbf{W}_v are weighting constants, and $C_{N|k}$ is the Jacobi constant at the end of the time horizon, computationally determined at time t_k . Note that both the predicted control input $\Delta \mathbf{v}_{i|k}$ and the time instants at which thrusters fire $T_{i|k}$ are optimization variables.

Due to the complexity of space dynamics, and being cognizant of the fact that terminal equality constraints can cause stability problems, we cannot ensure stability of our approach without severely limiting fuel savings; therefore we take N to be sufficiently large to be able to predict any large exogenous forces that would affect system stability. We also utilize the weight α for this same purpose, to trade off between optimizing fuel consumption ($\alpha = 1$) and tracking the nominal trajectory ($\alpha < 1$), expecting that good trajectory tracking would ensure stable behavior.

We solve (9) for $\Delta \mathbf{v}_k$, using the interior point optimization solver IPOPT (Wächter, 2002). In particular, our algorithm is implemented by connecting the trajectory at patch-points $t_{1|k}, \dots, t_{n-1|k}$ corresponding to indexes $i = 1, \dots, n - 1$, respectively. Since gradients of the cost functional as well as the Jacobian of the constraint vector are functions of the state transition matrix propagated between two intermediate patch points, we are able to provide user-defined objective gradients and constraint-Jacobians to boost the performance of the optimization algorithm.

4. RESULTS

In this section, we present results of numerical simulations that test our station-keeping schemes. Each simulation consists of Monte Carlo runs, for which we compute the mean and standard deviation of fuel consumption. In simulation, position measurement uncertainties are assumed

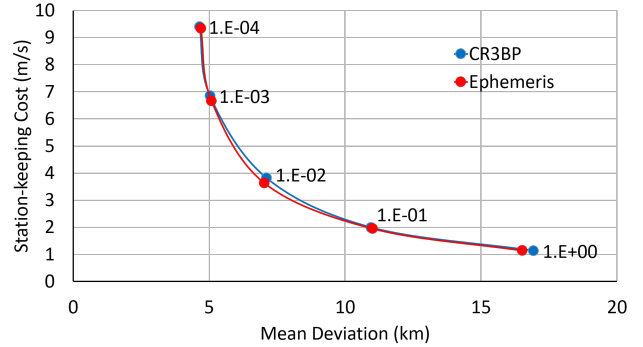


Fig. 2. 30-day trajectory tracking station-keeping cost plotted against mean deviation

to be unbiased with a standard deviation $\sigma = 0.1\text{km}$ in all three directions; velocity measurement uncertainties are also unbiased and have standard deviation $\sigma = 1\text{cm/s}$, resulting in $\mathbf{W}_k := \text{diag}(0.1, 0.1, 0.1, 1, 1, 1)$. We perform maneuvers at a rate of one every 7.6 hours, which corresponds to about one maneuver per revolution. This has been done because performing more than or less than one maneuver during the same orbit has not shown any improvement in tests under similar conditions (Muralidharan et al., 2020). Maneuvers spaced too far from each other may increase the overall station-keeping cost as it allows ample time for the spacecraft to deviate from the baseline trajectory.

4.1 Trajectory-tracking

We first consider the trajectory-tracking method, where the penalty matrix is chosen to be $\mathbf{R}_k = r\mathbf{I}_3$. We performed a test of different choices of r , running Monte Carlo simulations consisting of 100 runs each, and provide the results in Table 1 and Figs. 2 and 3, which correspond to both the CR3BP model dynamics and the more precise ephemeris model. Fig. 2 shows the relationship between station-keeping cost and the mean deviation computed for a one-month mission duration around the reference orbit for different choices of r . The results show that, when $r \leq 10^{-3}$, the spacecraft maintains a tight adherence to the reference trajectory but consumes a large amount of fuel while, when $r \geq 10^0$, the fuel consumption is at least 5 times better while the tracking is very poor, eventually resulting in the spacecraft losing track of the reference trajectory. Note that the difference in results obtained by the CR3BP and ephemeris models is small, which signifies a consistency between the two.

4.2 Neighborhood station-keeping

We now consider the alternative, neighborhood station-keeping scheme. This scheme, unlike the trajectory-tracking technique, uses a full, nonlinear model to determine maneuvers. The use of nonlinear dynamics increases the computational burden, which can be managed by choice of the time horizon N . To keep the computation reasonably fast, and in order to be able to simulate one month of station-keeping in less than one day on an ordinary desktop computer, we performed some numerical experiments and chose a bound $N \leq 5$, roughly corresponding to a length of 5 orbits, or a little more than 1.5 days. To achieve lower fuel consumption, we front-loaded the cost

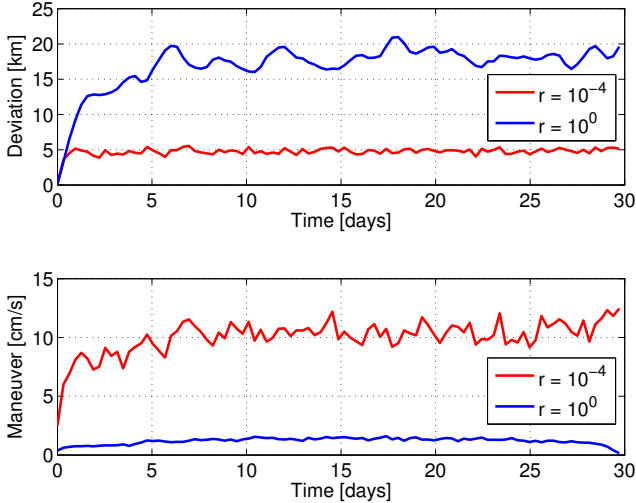


Fig. 3. Plot of trajectory tracking mean deviation and station-keeping cost plotted for $r = 10^{-4}$ (red) and $r = 10^0$ (blue)

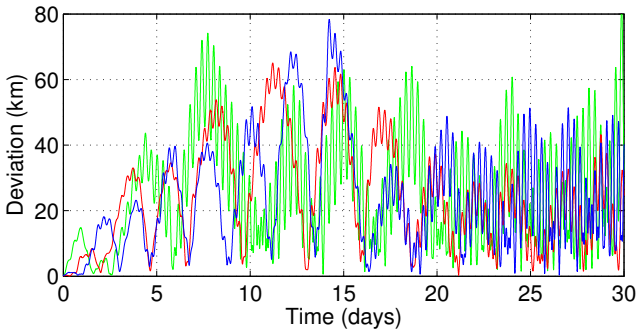


Fig. 4. Deviation from baseline trajectory for three separately colored, randomized runs corresponding to neighborhood station-keeping with $\alpha = 1$

on the initial control inputs; instead of using a decaying cost of the form $\xi_{k+1} = \gamma\xi_k$ for some positive $\gamma < 1$, we simply set $\xi_0 = 10$ and $\xi_k = 1$ for all other k . The higher ξ_0 increases the cost of the first maneuver; a lower one improves tracking but increases fuel cost.

Using the CR3BP model, we performed three sets of Monte Carlo simulations consisting of 20 runs each, corresponding to different choices of weight on fuel consumption $\alpha = 0, 0.5$ and 1 , results of which are tabulated in Table 2. The minimum-fuel solution, corresponding to $\alpha = 1$, had a fuel cost below the minimum fuel cost achieved using the trajectory-tracking technique. This improved value was obtained at the price of loosened station-keeping, as shown in Fig. 4, which exhibits the deviation of the optimal solution for three different sample trajectories corresponding to solving the optimization problem with $\alpha = 1$. Although the trajectories have larger deviations from the reference, they do maintain the same geometry as the reference and, despite large deviations, the spacecraft repeatedly approaches the baseline solution, suggesting that a relatively low-cost maneuver can always be implemented to put the spacecraft back on the reference trajectory. Fig. 5 shows a comparison of two trajectories corresponding to $\alpha = 0$ and 1 . The tight station-keeping solution in Fig. 5, obtained

Table 2. 30-day neighborhood station-keeping fuel cost for different choices of N

α	N	mean (m/s)	std. dev (1σ) (m/s)
1	2	0.45	0.49
	3	0.78	0.46
	4	0.86	0.48
	5	0.73	0.38
0.5	2	3.04	0.49
	5	4.56	0.46
0	5	8.07	0.47

using $\alpha = 0$, is comparable to the station-keeping results achieved by using the trajectory-tracking technique with r set to 10^{-4} .

We performed additional simulations to refine our choice for the time horizon N . Although a direct comparison cannot be made between these results and the trajectory-tracking scheme, the results, available in Table 2, show a consistent improvement in fuel consumption when using the former. Additionally, to showcase the versatility of this approach, we performed simulations corresponding to $\alpha = 0.5$, and the results are also available in Table 2. As expected, an intermediate value of α such as 0.5 results in intermediate station-keeping cost and deviation.

Jacobi constant in the ephemeris model: In the case of a higher fidelity model, in addition to the position states, velocity states, and time of propagation, the epoch time is also a dependent variable and hence it must also be incorporated into the design vector. The Jacobi constant is not constant in this model but the variable, computed according to (2), remains bounded along the reference trajectory, as shown in Fig. 6. The bounded Jacobi values indicate the bounded nature of the reference trajectory. In contrast to matching the Jacobi constant at the N -th node in the circular restricted model, in the higher fidelity case we instead match the Jacobi constant determined at the end of the horizon, *i.e.*, we modify (9d) to,

$$C_{N|k} = C_{\text{ref}}(t_{N|k}),$$

where $C_{\text{ref}}(t)$ corresponds to the reference trajectory Jacobi constant. Setting $N = 2$, using this approach, we obtain a 30-day fuel cost of 0.55m/s with α as 1 , and 7.33m/s with $\alpha = 0$.

4.3 Discussion

The results clearly show that both approaches can be modified to achieve low fuel consumption or good station keeping. The trajectory-tracking approach achieves acceptable tracking even at low fuel consumption, while neighborhood station-keeping, although staying in the neighborhood, does not exhibit close tracking. For this reason, the former method is recommended for ordinary scientific exploration, but the latter can still be useful in situations where considerations of fuel consumption are most important, *i.e.*, where we need to minimize fuel and hence set $\alpha = 1$. Such a situation can arise in emergencies or system failure.

5. CONCLUSION

In this work, we explored station-keeping on the QSO around Mars's moon, Phobos. We considered two kinds of

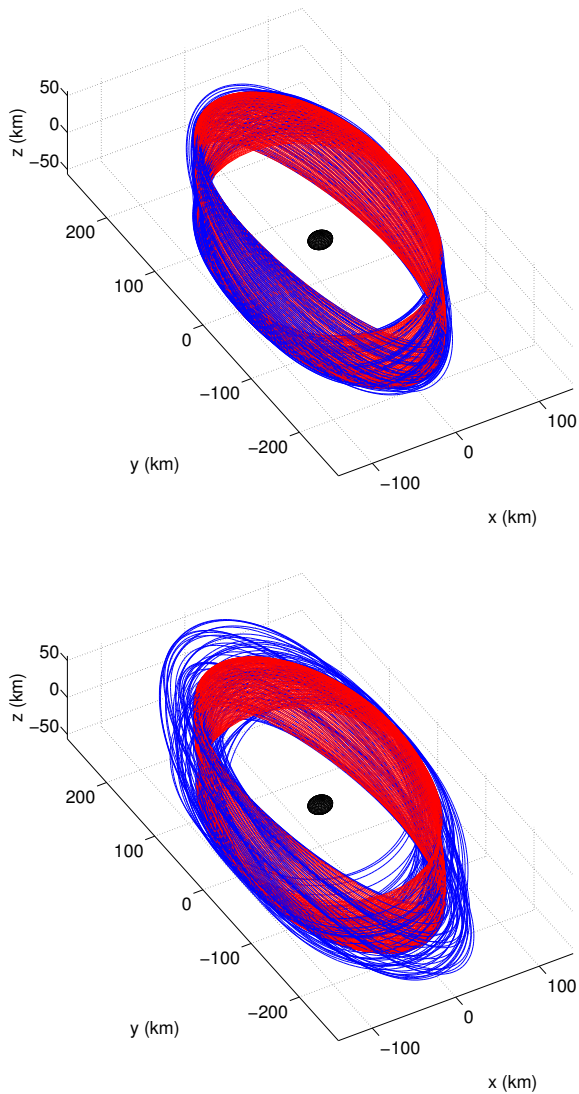


Fig. 5. Neighborhood station-keeping trajectories (blue) plotted against the reference orbit (red) for $\alpha = 0$ (top) and $\alpha = 1$ (bottom)

station-keeping schemes; one was based on linear dynamics with the goal of close tracking and the other was based on nonlinear dynamics with the goal of stabilizing to the manifold determined by a desired Jacobi constant. The trajectory-tracking method results in lower fuel consumption when the tracking is accurate. Because it is free to track trajectories with the same Jacobi constant as the reference trajectory, stabilization to the manifold provides better fuel consumption overall at the expense of close tracking. For this reason, we recommend this technique for orbit maintenance with a strict fuel savings requirement.

REFERENCES

Campagnola, S. et al. (2018). Mission analysis for the Martian Moons Explorer (MMX) mission. *Acta Astronaut.*, 146, 409–417.

Capdevila, L.R. (2016). *A transfer network linking Earth, Moon, and the triangular libration point regions in the Earth-Moon system*. Ph.D. thesis, Purdue Univ., West Lafayette, IN.

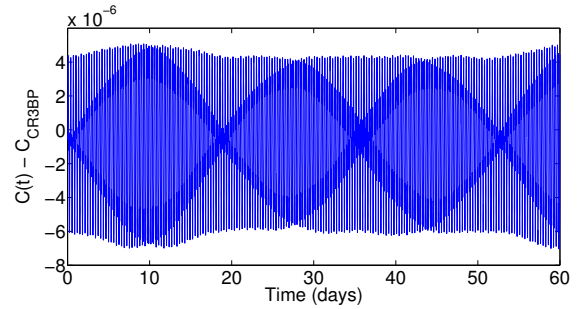


Fig. 6. Jacobi value deviation from nominal Jacobi constant in simulation using the ephemeris model

Çelik, O. et al. (2019). Ballistic deployment from quasi-satellite orbits around Phobos under realistic dynamical and surface environment constraints. *Planet. Space Sci.*, 178(104693).

Folkner, W.M. et al. (2009). The planetary and lunar ephemeris DE 421. The Interplanetary Network Progress Report 42-178.

Helfrich, C. et al. (2015). A journey with MOM. In *Proc. Int. Symp. Space Flight Dynamics*. Munich.

Howell, K.C. and Pernicka, H.J. (1988). Numerical determination of Lissajous trajectories in the restricted three-body problem. *Celest. Mech.*, 41, 107–124.

Jacobson, R.A. et al. (2018). The rotational elements of Mars and its satellites. *Planet. Space Sci.*, 152, 107–115.

Jakosky, B.M. et al. (2015). The Mars Atmosphere and Volatile Evolution (MAVEN) mission. *Space Sci. Rev.*, 195, 3–48.

Kolemen, E. et al. (2007). Quasi-periodic orbits of the restricted three-body problem made easy. In *AIP Conf. Proc.*, volume 886, 68–77.

McCarthy, B.P. (2019). *Characterization of Quasi-Periodic Orbits for Applications in the Sun-Earth and Earth-Moon Systems*. Master’s thesis, Purdue Univ., West Lafayette, IN.

Muralidharan, V. (2017). *Orbit Maintenance Strategies for Sun-Earth/Moon Libration Point Missions: Parameter Selection for Target Point and Cauchy-Green Tensor Approaches*. Master’s thesis, Purdue Univ., West Lafayette, IN.

Muralidharan, V. et al. (2020). Control strategy for long-term station-keeping on near-rectilinear halo orbits. In *Proc. AIAA SciTech Forum and Expo.*, 2020-1459. Orlando, FL.

Perozzi, E. and Ferraz-Mello, S. (eds.) (2016). *Space Manifold Dynamics*. Springer, New York.

Shirobokov, M. et al. (2017). Survey of station-keeping techniques for libration point orbits. *J. Guid. Control Dyn.*, 40(5), 1085–1105.

Stengel, R.F. (1994). *Optimal Control and Estimation*. Dover, Mineola, NY, 2nd edition.

Szebehely, V. (1967). *Theory of Orbit: The Restricted Problem of Three Bodies*. Academic Press, New York.

Wächter, A. (2002). *An interior point algorithm for large-scale nonlinear optimization with applications in process engineering*. Ph.D. thesis, Carnegie Mellon Univ., Pittsburgh.

Zurek, R.W. and Smrekar, S.E. (2007). An overview of the Mars Reconnaissance Orbiter (MRO) science mission. *J. Geophys. Res. Planets*, 112(E5S01).